Wireless multi-hop networks with stealing: large buffer asymptotics

Fabrice Guillemin
Orange Labs

Charles Knessl
University of Illinois at Chicago

Johan S.H. van Leeuwaarden
Eindhoven University of Technology

***Abstract*—Wireless networks equipped with CSMA are scheduled in a fully distributed manner. A disadvantage of such distributed control in multi-hop networks is the hidden node problem that causes the effect of *stealing*, in which a downstream node steals the channel from an upstream node with probability p. Aziz, Starobinski and Thiran [2] have recently shown that the N-hop model with stealing is stable only in the case $N = 3$ and $p \in (0, 1]$. This 3-hop model can be modeled as a random walk in the quarter plane. We derive various asymptotic expressions for the stationary large buffer probabilities of the 3-hop model that capture the effect of p.**

I. Introduction

Efficient usage of wireless networks requires decentralized protocols for transmitting data. In wireless mesh networks, most Medium Access Control (MAC) protocols use Carrier-Sense Multiple-Access (CSMA), and indeed CSMA schedules the capacity of the network in a distributed manner. The majority of protocols, however, has been developed for single-hop communication, while multi-hop scenarios, in which multiple links are used to transmit a packet from source to destination, are becoming ever more prominent.

CSMA builds upon the ALOHA protocol, in which nodes wait for some random back-off period before starting a transmission. The length of this back-off period is independent between nodes, ruling out a collision caused by multiple transmissions starting simultaneously. Nevertheless, a collision may occur in case a node activates during another node's transmission. The CSMA protocol prescribes that nodes should sense their surroundings for other transmitting nodes. If a node detects a nearby transmitter (within its sensing range), the back-off timer is frozen, deferring the countdown until the channel is sensed clear. Using this mechanism, the number of collisions is greatly reduced. However, CSMA introduces the additional problem of hidden nodes (see [13]). Hidden nodes are not detected by the carrier-sensing mechanism, but may still cause collisions. The hidden nodes give rise to the phenomenon of *stealing*, which can be best explained in the context of a multi-hop network with $N + 1$ nodes. Node 0 (the source) always has traffic to send. This traffic is sent to node N (the destination) and will be relayed through nodes $1, \ldots, N-1$. Both the transmission range and the interference range are limited to nearest neighbors. We assume that the network operates under the CSMA protocol, and that nodes have large buffers (with is usually the case). In fact, we assume infinite buffers, so that the network is lossless. Non-zero propagation delays and the hidden node problem will now give rise to the stealing effect.

The stealing effect occurs when a downstream node $i + 2$ captures the channel from an upstream node i, even though it accesses the medium later. Denote the probability of occurrence of stealing by p. Figure 1 gives an example of the hidden node problem and stealing for $N = 3$. Node 0 is transmitting to node 1, and hence node 1 is silenced. However, node 2 is not silenced, and when it decides to start transmitting to the destination node 3, this transmission will cause the ongoing transmission from node 0 to node 1 to fail.

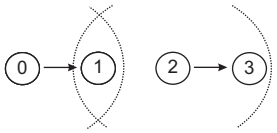

Fig. 1. The hidden node problem.

The assumption of infinite buffers (and no losses) gives rise to a potential stability problem, because the buffer contents may become infinite. A striking feature of stealing is that it can have a positive effect on stability. Indeed, in [2] it is shown that the 3-hop model without stealing ($p = 0$) is unstable, while the 3-hop model is stable if the stealing phenomenon occurs (when $p \in (0, 1]$). Hence, stealing has a positive influence in that it leads to a stable system. However, in [2] it is also shown that 4-hop networks are always unstable, even with stealing, and numerical evidence is provided that instability extends to larger networks. This makes the 3-hop network with stealing special, being the only stable multi-hop network, particularly when one realizes that more complex topologies are likely to contain such linear 3-hop segments. We shall restrict to the 3-hop network, and focus on the stationary distribution. In particular, we shall investigate the impact of the stealing parameter p on the large buffer asymptotics. Knowledge of the occurrence of such rare events provides structural insights into the behavior of the network and the impact of stealing, and are therefore of interest for dimensioning purposes.

In IEEE 802.11 stealing refers to the event that node $i + 2$ captures the channel despite a larger back-off value than node i, see [2]. Stealing will be absent ($p = 0$) only in the unrealistic scenario where the so-called RTS/CTS control messages are instantaneous, while the stealing would be perfect ($p = 1$) if the control messages are disabled. We shall consider both

the extreme scenarios $p = 0$ and $p = 1$. The true value for p depends on the protocol and messaging, and lies in the interval $(0, 1)$; see [2], [12].

We proceed as follows. In Section II we model the 3-hop network as a two-dimensional Markov chain, and show that it falls into the class of *random walks in the quarter plane*. We also provide simulation results that demonstrate the crucial impact that the stealing parameter p has on the evolution of the buffer contents. We then present our main findings in Section III, where we start in Section III-A with *perfect stealing* ($p = 1$). It that case, the two-dimensional Markov chain has a surprisingly simple product form solution. In Section III-B we consider the situation with a *small stealing effect* ($p \to 0$). For this, we identify a scaling limit of the Markov chain. This scaling limit turns out to be a continuous process in the positive quadrant that admits a simple product form solution for its stationary density. In Section III-C we present our key results that give the joint large buffer asymptotics for all $p \in (0, 1)$. Due to space limitations, we shall refer to the extended version [10] of this manuscript for several proofs and further details.

In proving the joint asymptotics in Section IV, we shall use the ray method of geometrical optics. While this will not yield the complete asymptotics, we will show that much of the basic structure can be inferred solely from the balance equations. The singular perturbation approach does make certain assumptions about the forms of the asymptotic expansions, and the asymptotic matching between different scales. In [10] we relate our approach to the compensation approach [1] and to singularity analysis [7], [8], [9], [11].

II. The 3-hop network

In this section we shall describe how the 3-hop network can be modeled as a two-dimensional Markov chain, following [2]. Consider a linear topology of four nodes. All packets are generated by node 0 and forwarded to node 3 by successive transmissions via the intermediate nodes 1 and 2 (see Figure 1). We assume that node 0 is saturated, so that there are always packets to be transmitted. The interference range of each node is taken to be nearest neighbors, which for this 3-hop network implies that only one of the first three nodes can be active at a given time slot. Each node is assumed to have an infinite buffer for storage of data packets.

In the case of idealized CSMA/CA without stealing (see [2]), all non-empty nodes have exactly the same probability of being scheduled. When all three nodes have non-empty buffers, each node has a success probability of 1/3. When only nodes 0 and 1 (or nodes 0 and 2) are non-empty, their success probabilities are 1/2, and when nodes 1 and 2 are both empty, a packet will be transmitted from node 0 to node 1 with probability 1. The stealing effect describes a bias towards the downstream node 2. When only node 0 and 1 compete for the channel, the success probability of each node remains 1/2. However, when node 0 and 2 compete together, there is a probability p that node 2 steals the channel.

Denoting by $N_k(\tau)$ the number of packets at node k at the beginning of time slot τ, the two-dimensional process $\{(N_1(\tau), N_2(\tau)), \tau \in \mathbb{N}\}$ is a two-dimensional Markov chain, and in fact a random walk in the quarter plane, as depicted in Figure 2.

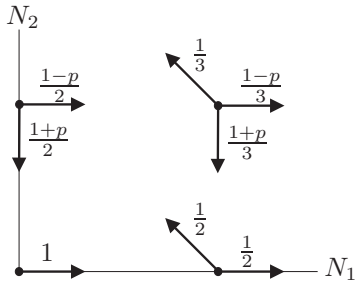

Fig. 2. The random walk in the quarter plane.

The random walk takes the following steps:

- In the interior of the state space, the walk steps $(1, 0)$ w.p. $\frac{1-p}{3}$, $(0, -1)$ w.p. $\frac{1+p}{3}$ and $(-1, 1)$ w.p. $\frac{1}{3}$.
- On the horizontal axis, the walk steps $(1, 0)$ w.p. $\frac{1}{2}$ and $(-1, 1)$ w.p. $\frac{1}{2}$.
- On the vertical axis, the walk steps $(1, 0)$ w.p. $\frac{1-p}{2}$ and $(0, -1)$ w.p. $\frac{1+p}{2}$.

The stability condition under which this random walk is ergodic, and thus has a unique stationary distribution, was proved in [2] using Foster's criterion and a Lyapunov function:

Proposition 1: (Aziz, Starobinski and Thiran [2]) The random walk $\{(N_1(\tau), N_2(\tau)), \tau \in \mathbb{N}\}$ is ergodic if and only if $p \in (0, 1]$.

Denote the joint stationary probabilities by $\pi(n, k) = \mathbb{P}(N_1 = n, N_2 = k) = \lim_{\tau\to\infty} \mathbb{P}(N_1(\tau) = n, N_2(\tau) = k)$. The balance equations for the interior of the state space read

$$\begin{aligned}\pi(n,k) =& \frac{1}{3}\pi(n+1,k-1) + \frac{1-p}{3}\pi(n-1,k) \\ &+ \frac{1+p}{3}\pi(n,k+1), \quad n,k \geq 2, \qquad (1)\\ \pi(n,1) =& \frac{1}{2}\pi(n+1,0) + \frac{1-p}{3}\pi(n-1,1) \\ &+ \frac{1+p}{3}\pi(n,2), \quad n \geq 2, \qquad (2)\\ \pi(1,k) =& \frac{1}{3}\pi(2,k-1) + \frac{1-p}{2}\pi(0,k) \\ &+ \frac{1+p}{3}\pi(1,k+1), \quad k \geq 2, \qquad (3)\end{aligned}$$

while on the boundaries we have

$$\pi(n,0) = \frac{1+p}{3}\pi(n,1) + \frac{1}{2}\pi(n-1,0), \quad n \geq 2, \qquad (4)$$

$$\pi(0,k) = \frac{1}{3}\pi(1,k-1) + \frac{1+p}{2}\pi(0,k+1), \quad k \geq 2, \qquad (5)$$

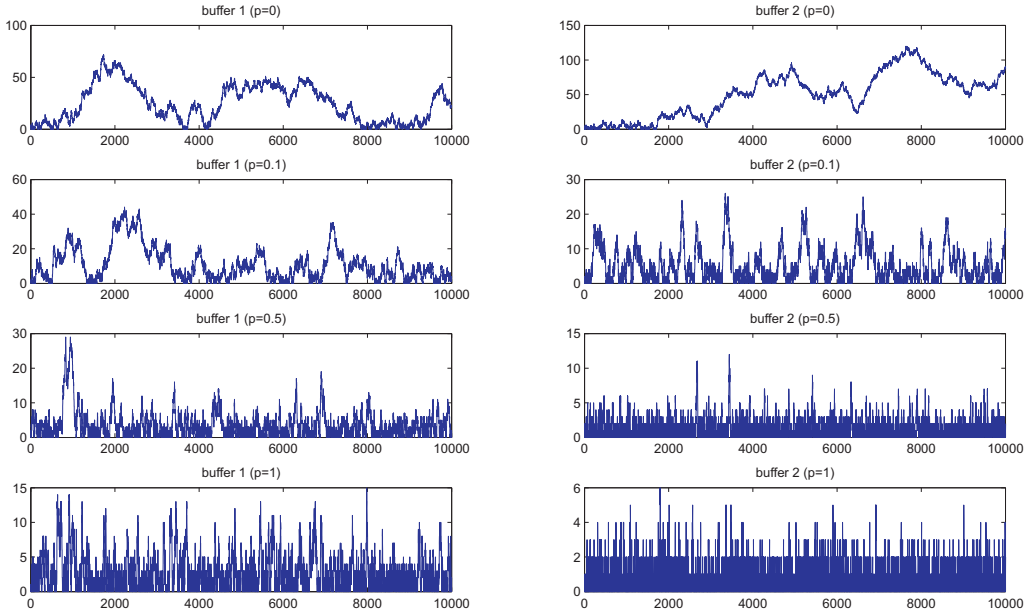

Fig. 3. Buffer evolution for the 3-hop model for 10,000 slots and various stealing probabilities p.

and

$$\pi(1,0) = \frac{1+p}{3}\pi(1,1) + \pi(0,0), \tag{6}$$

$$\pi(0,1) = \frac{1}{2}\pi(1,0) + \frac{1+p}{2}\pi(0,2), \tag{7}$$

$$\pi(0,0) = \frac{1+p}{2}\pi(0,1). \tag{8}$$

Let $P(x,y)$ represent the bivariate generating function

$$P(x,y) = \sum_{n=0}^{\infty}\sum_{k=0}^{\infty}\mathbb{P}(N_1 = n, N_2 = k)x^n y^k.$$

From the balance equations it follows that $P(x,y)$ satisfies the functional equation

$$h_1(x,y)P(x,y) = h_2(x,y)P(x,0) + h_3(x,y)P(0,y) + h_4(x,y)P(0,0), \tag{9}$$

where

$$h_1(x,y) = 6xy - 2(1-p)x^2y - 2y^2 - 2(1+p)x, \tag{10}$$

$$h_2(x,y) = (1+2p)x^2y + y^2 - 2(1+p)x, \tag{11}$$

$$h_3(x,y) = (1-p)x^2y - 2y^2 + (1+p)x, \tag{12}$$

$$h_4(x,y) = (2+p)x^2y - y^2 - (1+p)x. \tag{13}$$

See [6], Section 1.3, for a general description of how to derive such functional equations. The functions h_j are quadratic polynomials in x or y. Equation (9) cannot be solved directly for $P(x,y)$, because it contains other unknown functions $P(x,0)$ and $P(0,y)$. The approach is then to consider the roots of the kernel $h_1(x,y)$ w.r.t. one of the variables x, y. Substituting such roots into (9) yields additional equations between the unknowns $P(x,0)$ and $P(0,y)$ that are free of the term containing the full generating function $P(x,y)$. These additional equations in fact give rise to boundary value problems whose solutions lead to a specification of $P(x,0)$ and $P(0,y)$ and hence $P(x,y)$. Hence, stationary distributions of two-dimensional one-step random walks in the quarter plane can be obtained by solving functional equations (see [5], [6]). For the present model this will be done in [11].

A. The effect of stealing

Let us now consider the effect of stealing on the evolution of the buffer contents of node 1 and node 2. Results from our simulation are displayed in Figure 3. Several interesting observations can be made. First, the sizes of both buffers decrease with p. The case $p = 0$ is critical, leading to large fluctuations. As the stealing becomes more dominant, the buffer contents decrease. Second, the buffer of node 1 seems to be roughly twice as large as the buffer of node 2. Third, the regeneration periods, defined as the periods between two consecutive times that the buffer empties, tend to become shorter as p increases.

In this paper we shall focus on the occurrence of large buffer contents, that can be considered as *rare events*. We will derive asymptotic expressions for the probabilities of large buffer contents. It is clear from Figure 3 that large buffer contents become more likely as p becomes smaller, and that large buffer contents are more likely to occur at node 1 than at node 2. The latter is because the stealing effect favors the downstream node. To substantiate these numerical observations, we shall derive asymptotic expressions for the probabilities that the buffer contents become large.

We will obtain the asymptotic results directly from the balance equation in (1)-(8) by using the so-called ray method. In a companion paper [11] we take a different approach, making use of the exact solution to the functional equation (9). Solving the functional equation requires sophisticated complex analysis, and the obtained formal solution is too complicated to invert directly for the stationary distribution. That is why in [11] we employ the functional equation (9) to determine the dominant (closest to the origin) singularities of the function $P(x,y)$. Subsequently, by investigating $P(x,y)$ in the neighborhood of these dominant singularities, and by the asymptotic evaluation of complex integrals, we obtain asymptotic expressions for the tail of the probability distribution of (N_1, N_2). This approach is sketched in [10].

III. Main results

In this section we shall present results for the case of perfect stealing ($p = 1$), the case of a small stealing effect ($p \approx 0$), and then the general case $p \in (0,1)$.

A. Perfect stealing

For the case of perfect stealing, where $p = 1$ and hence node 2 always steals the channel, the random walk becomes more tractable. Visual inspection of Figure 2 tells us that the walk can no longer step to the East in the interior of the state space. As it turns out, the random walk allows for a simple product form solution for its stationary distribution.

Theorem 1: For the case $p = 1$ the stationary distribution of the random walk has a closed-form solution with $\pi(0,0) = \pi(0,1) = (2-\sqrt{2})/6$, $\pi(1,0) = (\sqrt{2}-1)/3$ and

$$\pi(n,k) = \left(\frac{1}{\sqrt{2}}\right)^n \left(1-\frac{1}{\sqrt{2}}\right)^{k+1}, \quad n,k \geq 1, \tag{14}$$

$$\pi(n,0) = \frac{2}{3}\left(1-\frac{1}{\sqrt{2}}\right)\left(\frac{1}{\sqrt{2}}\right)^n, \quad n \geq 1, \tag{15}$$

$$\pi(0,k) = \frac{1}{3}\left(1-\frac{1}{\sqrt{2}}\right)^k, \quad k \geq 1. \tag{16}$$

Theorem 1 is proved in [10]. The marginal distribution follows from Theorem 1:

Corollary 1: For the case $p = 1$ we have the marginal distributions

$$\mathbb{P}(N_1 = n) = \frac{7\sqrt{2}-8}{6}\left(\frac{1}{\sqrt{2}}\right)^n, \quad n \geq 1, \tag{17}$$

$$\mathbb{P}(N_2 = k) = \left(\frac{1}{3}+\frac{1}{\sqrt{2}}\right)\left(1-\frac{1}{\sqrt{2}}\right)^k, \quad k \geq 1, \tag{18}$$

$\mathbb{P}(N_1 = 0) = \sqrt{2}/6$ and $\mathbb{P}(N_2 = 0) = (2+\sqrt{2})/6$.
Note that $\mathbb{P}(N_2 = k)$ decays faster than $\mathbb{P}(N_1 = n)$, so that large buffer contents are more likely to occur at node 1.

B. Small stealing effect

We now turn to the case $p \approx 0$, so that the probability that node 2 steals the channel is small. Using the right space-time scaling, we show in [10] that our random walk in the quarter plane converges to a continuous scaling limit whose stationary density obeys a PDE with a simple product form solution. The result is as follows:

Theorem 2: For the case $p \to 0$, the stationary distribution of the random walk can be approximated as

$$\pi(n,k) \approx p^2 \mathcal{G}(pn, pk), \quad n,k \geq 1, \tag{19}$$

$$\pi(n,0) \approx \frac{2}{3}p^2 \mathcal{G}(pn, 0), \quad n \geq 1, \tag{20}$$

$$\pi(0,k) \approx \frac{2}{3}p^2 \mathcal{G}(0, pk), \quad k \geq 1, \tag{21}$$

$$\pi(0,0) \approx \frac{1}{3}p^2 \mathcal{G}(0,0), \tag{22}$$

where the density $\mathcal{G}(X,Y)$ satisfies the PDE

$$\mathcal{G}_{XX} + \mathcal{G}_{YY} - \mathcal{G}_{XY} + \mathcal{G}_X + \mathcal{G}_Y = 0; \quad X,Y > 0, \tag{23}$$

with the boundary conditions

$$\mathcal{G}_X(0,Y) + \mathcal{G}(0,Y) = 0, \tag{24}$$

$$\mathcal{G}_X(X,0) - \mathcal{G}_Y(X,0) - \mathcal{G}(X,0) = 0, \tag{25}$$

and with normalized solution

$$\mathcal{G}(X,Y) = 2\mathrm{e}^{-X}\mathrm{e}^{-2Y}. \tag{26}$$

The marginal distributions then readily follow:

Corollary 2: For $p \to 0$ we have the approximative marginal distributions

$$\mathbb{P}(N_1 = n) \approx p\mathrm{e}^{-pn}, \quad n \geq 1, \tag{27}$$

$$\mathbb{P}(N_2 = k) \approx 2p\mathrm{e}^{-2pk}, \quad k \geq 1, \tag{28}$$

$\mathbb{P}(N_1 = 0) \approx \frac{2}{3}p$ and $\mathbb{P}(N_2 = 0) \approx \frac{4}{3}p$.
Note that $\mathbb{P}(N_2 = k)$ decays precisely twice as fast as $\mathbb{P}(N_1 = n)$. Theorem 2 and Corollary 2 provide approximations for the stationary distribution of the random walk that are sharp for small values of p. An example is given in Table I. The "true" values for $\mathbb{P}(N_1 = n)$ and $\mathbb{P}(N_2 = n)$ that are reported in Table I (and in all other tables in this paper) are obtained by numerical calculations. Truncating the state space by imposing an upper bound on one of the buffers reduces the random walk in the quarter plane to a random walk on an infinite strip, better known as a Quasi-Birth-Death (QBD) chain. For these Markov chains, fast numerical algorithms are available (see [15]). All numerical results presented were obtained by imposing an upper bound on the second buffer of 500.

C. Joint asymptotics

We now present results for the asymptotics of the stationary probabilities $\pi(n,k)$, for a fixed $0 < p < 1$ and n and/or $k \to \infty$. The results presented will be proved in Section IV using a singular perturbation approach for approximating the difference equations (1)-(5), and in particular the ray method of geometrical optics.

Theorem 3: For $n \to \infty$ and/or $k \to \infty$ there holds

$$\pi(n,k) \sim C \cdot B^k \left(A^n + \gamma A_*^n\right), \quad n,k \geq 1, \tag{29}$$

$$\pi(n,0) \sim C \cdot \frac{2}{3} \cdot A^n, \tag{30}$$

$$\pi(0,k) \sim C \cdot \frac{2}{3} \cdot (1+\gamma) B^k, \tag{31}$$

n	$\mathbb{P}(N_1 = n)$	$p\exp(-pn)$	$\mathbb{P}(N_2 = k)$	$2p\exp(-2pk)$
5.0000e+00	9.3641e-03	9.5123e-03	1.7892e-02	1.8097e-02
1.0000e+01	8.9136e-03	9.0484e-03	1.6211e-02	1.6375e-02
1.5000e+01	8.4849e-03	8.6071e-03	1.4686e-02	1.4816e-02
2.0000e+01	8.0769e-03	8.1873e-03	1.3302e-02	1.3406e-02
5.0000e+01	6.0099e-03	6.0653e-03	7.3397e-03	7.3576e-03
1.0000e+02	3.6722e-03	3.6788e-03	2.7198e-03	2.7067e-03

TABLE I
MARGINAL DISTRIBUTIONS AND THEIR APPROXIMATIONS IN (27) AND (28) FOR $p = 0.01$.

with C a constant, and

$$A = \frac{1 - p + \sqrt{1 + 2p + 5p^2}}{2(1 + p)}, \tag{32}$$

$$B = \frac{1 + 3p - \sqrt{1 + 2p + 5p^2}}{2p(1 + p)}, \tag{33}$$

$$A_* = \frac{(1 - p)(-1 - p + \sqrt{1 + 2p + 5p^2})}{2p^2}, \tag{34}$$

$$\gamma = \frac{2p^2 - 1 - p + \sqrt{1 + 2p + 5p^2}}{2p(1 + p)}. \tag{35}$$

The constant $C = C(p)$ satisfies $C(1) = 1-1/\sqrt{2}$ and $C(p) \sim 2p^2$ as $p \to 0$.

It is readily seen that $A > B > A_*$ for all $p \in (0, 1]$, which again confirms the fact that large buffers are more likely at node 1. From (32) and (33) we further see that $A = 1/\sqrt{2}$ and $B = 1 - 1/\sqrt{2}$ when $p = 1$, which agrees with Theorem 1. The functions A, B and A_* are plotted in Figure 4.

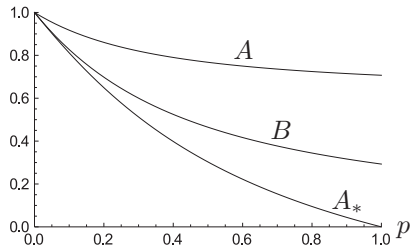

Fig. 4. The decay rates A, B and A_* for $p = (0, 1]$.

Some further calculations lead to the following asymptotic result for the marginals:

Corollary 3: For the marginal distributions we find the asymptotic relations

$$\mathbb{P}(N_1 = n) \sim C \left(\frac{2}{3} + \frac{B}{1 - B} \right) A^n, \quad n \to \infty, \tag{36}$$

$$\mathbb{P}(N_2 = k) \sim C \left(\frac{2}{3}(1 + \gamma) + \frac{A}{1 - A} + \gamma \frac{A_*}{1 - A_*} \right) B^k, \tag{37}$$

as $k \to \infty$.

Several results that test the accuracy of (36) and (37) are provided in Tables II-IV. We see that in all cases the asymptotics kick in fast, which suggests that the asymptotic relations provide sharp approximations to the true values, even for small or moderate values of the buffer content.

n	$\mathbb{P}(N_1 = n)$	A^n	$\mathbb{P}(N_1 = n)A^{-n}$
5.0000e+00	7.0114e-02	3.7055e-01	1.8922e-01
1.0000e+01	2.5870e-02	1.3731e-01	1.8841e-01
1.5000e+01	9.5836e-03	5.0879e-02	1.8836e-01
2.0000e+01	3.5511e-03	1.8853e-02	1.8835e-01
5.0000e+01	9.1928e-06	4.8806e-05	1.8835e-01
1.0000e+02	4.4866e-10	2.3820e-09	1.8835e-01

TABLE II
MARGINAL DISTRIBUTION OF N_1 FOR $p = 0.3$.

n	$\mathbb{P}(N_1 = n)$	A^n	$\mathbb{P}(N_1 = n)A^{-n}$
5.0000e+00	5.7326e-02	1.8695e-01	3.0663e-01
1.0000e+01	1.0717e-02	3.4951e-02	3.0663e-01
1.5000e+01	2.0036e-03	6.5342e-03	3.0663e-01
2.0000e+01	3.7458e-04	1.2216e-03	3.0663e-01
5.0000e+01	1.5993e-08	5.2156e-08	3.0663e-01
1.0000e+02	8.3412e-16	2.7202e-15	3.0663e-01

TABLE III
MARGINAL DISTRIBUTION OF N_1 FOR $p = 0.9$.

k	$\mathbb{P}(N_2 = k)$	B^k	$\mathbb{P}(N_2 = k)B^{-k}$
5.0000e+00	3.1621e-03	3.1806e-03	9.9419e-01
1.0000e+01	1.0057e-05	1.0116e-05	9.9419e-01
1.5000e+01	3.1989e-08	3.2176e-08	9.9419e-01
2.0000e+01	1.0174e-10	1.0234e-10	9.9419e-01
5.0000e+01	1.0533e-25	1.0595e-25	9.9419e-01
1.0000e+02	1.1159e-50	1.1225e-50	9.9419e-01

TABLE IV
MARGINAL DISTRIBUTION OF N_2 FOR $p = 0.9$.

We next give some of the higher order terms in the asymptotic expansion of $\pi(n, k)$, which show the ultimate deviation from product form behavior.

Theorem 4: For $n, k \to \infty$, we define the ratio $R = k/n$. Then for $0 < R < \infty$ we have:
(i) If $0 < p < (5 - \sqrt{17})/2$, $R > \mathcal{S}_1(p)$,

$$\pi(n, k) \sim C \left(A^n B^k + \gamma A_*^n B^k + \frac{1}{\sqrt{n}} f(R)[a(R)]^n [b(R)]^k \right), \tag{38}$$

with

$$\mathcal{S}_1(p) = \frac{4p^2 - 11p - 1 + 3\sqrt{1 + 2p + 5p^2}}{2(1 + 2p - 4p^2)}, \tag{39}$$

and a and b are obtained from solving the system of equations

$$3 - \frac{1-p}{a} = \frac{a}{b} + (1+p)b, \tag{40}$$

$$R\left[\frac{1-p}{a} - \frac{a}{b}\right] = \frac{a}{b} - (1+p)b. \tag{41}$$

(ii) If $0 < p < (5-\sqrt{17})/2$, $0 < R < \mathcal{S}_1(p)$,

$$\pi(n,k) \sim C\left(A^n B^k + \frac{1}{\sqrt{n}} f(R)[a(R)]^n [b(R)]^k\right), \tag{42}$$

(iii) If $(5-\sqrt{17})/2 < p < 1$, $R > \mathcal{S}_2(p)$, with

$$\mathcal{S}_2(p) = \frac{2p^2 - p - 5 + 3\sqrt{1+2p+5p^2}}{2(2+4p+p^2)}, \tag{43}$$

then there is the asymptotics in (38).
(iv) If $(5-\sqrt{17})/2 < p < 1$, $0 < R < \mathcal{S}_2(p)$,

$$\pi(n,k) \sim C\Big(A^n B^k + \gamma A_*^n B^k + \delta A_*^n B_*^k + \frac{1}{\sqrt{n}} f(R)[a(R)]^n [b(R)]^k\Big) \tag{44}$$

with

$$B_* = \frac{(1-p)(p-1+\sqrt{1+2p+5p^2})}{2p(1+p)}, \tag{45}$$

$$\delta = \frac{1+2p^2+p^3-4p^4+(p^2+p-1)\sqrt{1+2p+5p^2}}{2p(p^4-p^2-p-1)}. \tag{46}$$

We ordered the terms in the right sides for π in Theorem 4 so that each term is exponentially smaller than the term that preceeds it ($A_* < A$ and $B_* < B$). We cannot obtain the function $f(R)$ explicitly, without having the full solution for $\pi(n,k)$. Later we shall discuss the behavior of $f(R)$, for $R \to 0$, $R \to \infty$ and $R \to \mathcal{S}_j(p)$. We can recast the systems of equations for (a,b) as

$$0 = (1+p)(R+2)^2 a^3 - 9(R+1)a^2 + 3(1-p)(2+2R-R^2)a + (1-p)(R-1)(2R+1), \tag{47}$$

$$b = \frac{3(R+1) - (1-p)(2R+1)a^{-1}}{(1+p)(R+2)}. \tag{48}$$

Thus, given $R = k/n$ and p, we must solve the above cubic equation (47) for a, and then compute b from (48). When $p = (5-\sqrt{17})/2$ we have $a(0) = A_* = (7-\sqrt{17})/8$ (and then $b = B = B_*$), when $R = \mathcal{S}_1(p)$ we have $a = A_*$ and $b = B$, and when $R = \mathcal{S}_2(p)$ we have $a = A_*$ and $b = B_*$. Also, when $p = (5-\sqrt{17})/2$, $\mathcal{S}_1 = \mathcal{S}_2 = 0$.

The formulas in Theorem 4 must be slightly modified if $k = O(1)$, $n \to \infty$; $n = O(1)$, $k \to \infty$ or $R \approx \mathcal{S}_j(p)$, $j = 1, 2$. We thus see that a fair amount of asymptotic information can be obtained without solving fully for $\pi(n,k)$, and that the solution is a mixture of 3 exponentials and the term $a^n b^k$, which is geometric for each fixed $R = k/n$, but not globally geometric. This term represents the second term in the asymptotic expansion of π for case (ii), the third term for the cases (i) and (iii), and only the fourth term for case (iv).

IV. Proofs of Theorems 3 and 4

In this section we give the proofs of Theorem 3 and Theorem 4 using the ray method. While the ray method will not yield the complete asymptotics, we will show that much of the basic structure can be inferred solely from the balance equations. We shall obtain the leading term up to a multiplicative constant, and then discuss some of the higher order terms. In the ray method we seek an asymptotic solution of (1) in the form

$$\pi(n,k) \sim \mathrm{e}^{\Phi(n,k)} L(n,k), \tag{49}$$

where Φ satisfies the "eiconal" equation

$$3 = \mathrm{e}^{\Phi_n - \Phi_k} + (1-p)\mathrm{e}^{-\Phi_n} + (1+p)\mathrm{e}^{\Phi_k} \tag{50}$$

and L satisfies the "transport" equation

$$0 = \mathrm{e}^{\Phi_n - \Phi_k}\left[L_n - L_k + \left(\frac{1}{2}\Phi_{nn} - \Phi_{nk} + \frac{1}{2}\Phi_{kk}\right)\right] + (1-p)\mathrm{e}^{-\Phi_n}\left[-L_n + \frac{1}{2}\Phi_{nn} L\right] + (1+p)\mathrm{e}^{\Phi_k}\left[L_k + \frac{1}{2}\Phi_{kk} L\right]. \tag{51}$$

We will see that Φ has linear growth in n, k, and L has algebraic growth, thus the asymptotic limit in (49) fails to satisfy (1) exactly only in that (51) neglects derivatives of L of order ≥ 2, and derivatives of Φ of order ≥ 3.

Equation (50) is a non-linear PDE of the first order, which can be solved by the method of characteristics. The characteristic curves, or "rays", can be obtained by solving the system

$$\dot{n} = (1-p)\mathrm{e}^{-\Phi_n} - \mathrm{e}^{\Phi_n - \Phi_k},$$
$$\dot{k} = \mathrm{e}^{\Phi_n - \Phi_k} - (1+p)\mathrm{e}^{\Phi_k}, \tag{52}$$

$$\dot{\Phi}_n = 0, \quad \dot{\Phi}_k = 0, \tag{53}$$

$$\dot{\Phi} = \Phi_n\left[(1-p)\mathrm{e}^{-\Phi_n} - \mathrm{e}^{\Phi_n - \Phi_k}\right] + \Phi_k\left[\mathrm{e}^{\Phi_n - \Phi_k} - (1+p)\mathrm{e}^{\Phi_k}\right]. \tag{54}$$

Here, "$\dot{\cdot} = \frac{d}{dt}$" denotes a derivative along a ray.

We consider three main families of rays: rays that start from the k-axis ($n = 0$), rays that start from the n-axis ($k = 0$), and rays that start from the origin $(n,k) = (0,0)$ at various slopes. We shall also consider the reflections of the first two ray families. The rays from the axes, as well as from their reflections, will lead to purely exponential solutions to (1).

First we consider rays from $k = 0$. These must take into account the boundary conditions in (2) and (4). Along $k = 0$ we allow for a discontinuity in (49), setting

$$\pi(n,0) \sim \mathrm{e}^{\Phi(n,0)} \tilde{L}(n), \tag{55}$$

Then, with (51) and (55), (2) leads to

$$L(n,0)\mathrm{e}^{\Phi_k(n,0)} = \frac{1}{2}\tilde{L}(n)\mathrm{e}^{\Phi_n(n,0)} + \Big[\frac{1-p}{3}\mathrm{e}^{\Phi_k(n,0) - \Phi_n(n,0)} + \frac{1+p}{3}\mathrm{e}^{2\Phi_k(n,0)}\Big] L(n,0), \tag{56}$$

and (4) gives

$$\tilde{L}(n) = \frac{1+p}{3}\mathrm{e}^{\Phi_k(n,0)}L(n,0) + \frac{1}{2}\mathrm{e}^{-\Phi_n(n,0)}\tilde{L}(n). \quad (57)$$

Using (50) with $k=0$ and comparing this to (56) we conclude that $\tilde{L}(n) = \frac{2}{3}L(n,0)$ and then (57) gives

$$\frac{2}{3} = \frac{1+p}{3}\mathrm{e}^{\Phi_k(n,0)} + \frac{1}{3}\mathrm{e}^{-\Phi_n(n,0)}, \quad (58)$$

which is the desired boundary condition for Φ along $k=0$.

We return to (52)-(54). From (53) we conclude that Φ_n and Φ_k are both constant along a ray, and we write $\Phi_n = \log A$ and $\Phi_k = \log B$. But the boundary condition in (58) implies that Φ_n and Φ_k are constant globally. Then we can solve for (A,B) by using (50) (i.e. $3 = A/B + (1-p)/A + (1+p)B$) and (58) (i.e., $2 = (1+p)B + 1/A$), which leads to (32) and (33).

We next determine the domain that is filled by the rays from the n-axis. Solving (52) leads to

$$n = n_0 + \left(\frac{1-p}{A} - \frac{A}{B}\right)t, \quad k = \left(\frac{A}{B} - (1+p)B\right)t, \quad (59)$$

which gives the rays in parametric form. Here, n_0 is where the ray begins on the n-axis. The rays must enter the state space $(n, k \geq 0)$ for $t > 0$, and it is easy to verify that, $\forall p \in (0,1]$,

$$\dot{k} = -1 - \frac{1}{2p} + \frac{p}{2} + \left(\frac{1}{2} + \frac{1}{2p}\right)\sqrt{1+2p+5p^2} > 0. \quad (60)$$

Furthermore, $\forall p \in (0,1]$,

$$\dot{n} = \frac{1}{2} - p - \frac{1}{2p} + \left(\frac{1}{2p} - 1\right)\sqrt{1+2p+5p^2} < 0, \quad (61)$$

so that the rays fill the entire quadrant. By considering in more detail the boundary condition for $L(n,k)$ along $k=0$ we can show that L is in fact a constant (it follows immediately from (51), since $\Phi_{nn} = \Phi_{kk} = \Phi_{nk} = 0$, that L is a constant along a ray). Also, (54) can be written as $\dot{\Phi} = (\log A)\dot{n} + (\log B)\dot{k}$ so that $\Phi = n\log A + k\log B$ and $\mathrm{e}^{\Phi} = A^n B^k$. We have thus shown that an asymptotic solution of (1), (2) and (4) is

$$\pi(n,0) \sim \frac{2}{3}CA^n, \quad \pi(n,k) \sim CA^n B^k, \ k \geq 1. \quad (62)$$

This fails to satisfy the boundary condition along $n=0$, cf. (3) and (5).

It remains to consider rays from the k-axis ($n=0$) and rays from the origin. But we can show that rays from the k-axis would correspond to a product from solution with $\dot{n} < 0$, so the corresponding ray family would not enter the domain. We shall discuss rays from the origin shortly, but these will lead to a solution exponentially smaller than (62).

To satisfy the boundary condition along $n=0$ and $n=1$ in (5) and (3) we must consider the scale $n = O(1)$, $k \to \infty$ and construct a "boundary layer" correction to (62). Since (62) is a product form this essentially corresponds to the second step of the compensation methods of Adan [1]. Setting $\pi(n,k) \sim B^k g(n)$ for $n \geq 1$ and $\pi(0,k) \sim B^k g_0$ and analyzing (1), (3) and (5), we find that $g(n)$ satisfies the simple difference equation

$$3 = B^{-1}g(n+1) + (1-p)g(n-1) + (1+p)Bg(n), \quad (63)$$

so that $g(n)$ is a linear combination of A^n and A_*^n (defined in (34)). Then (3) and (5) show that $g_0 = \frac{2}{3}g(0)$ and that $g(n)$ must be proportional to $A^n + \gamma A_*^n$ with γ in (35). Thus we have introduced the second exponential $B^k A_*^n$ into the solution. Also, we have $A > A_*$ for all p.

This second exponential can be interpreted in terms of the ray method, as the reflection (in the k-axis) of the rays that started in the n-axis. The reflected rays have

$$\dot{k} = \frac{A_*}{B} - (1+p)B = -\frac{1}{p} - \frac{1}{2} - \frac{p}{2} + \left(\frac{1}{p} - \frac{1}{2}\right)\sqrt{1+2p+5p^2} \quad (64)$$

and

$$\dot{n} = \frac{1-p}{A_*} - \frac{A_*}{B} = p + \frac{1}{2p} - \frac{1}{2} + \left(1 - \frac{1}{2p}\right)\sqrt{1+2p+5p^2}. \quad (65)$$

We have $\dot{n} > 0$ for all $p \in (0,1]$ so that the reflected rays enter the positive quadrant. However, we can have $\dot{k} > 0$ or $\dot{k} < 0$. From (64) we see that $\dot{k} = 0$ if $p = \frac{1}{2}(5 - \sqrt{17}) \equiv p_*$. Then we obtain $\dot{k} < 0$ for $p_* < p < 1$ and $\dot{k} > 0$ for $0 < p < p_*$. The reflected rays all have the same slope, that is the ratio of the right side of (64) to that of (65), and this is the same as $\mathcal{S}_1(p)$ in (39). For $0 < p < p_*$ the reflected rays fill only the sector $k/n > \mathcal{S}_1(p)$, while if $p_* < p < 1$, they fill the entire positive quadrant. In the latter case the reflected rays are themselves reflected in the n-axis ($k=0$). This corresponds to a secondary reflection of the rays that started in the n-axis, and this will lead to a third exponential appearing in the solution as p increases past p_*. For $p < p_*$ only the two exponentials $A^n B^k$ and $A_*^n B^k$ appear. But then there is the transition in the asymptotics of $\pi(n,k) - CA^n B^k$ along the ray $k/n = \mathcal{S}_1(p)$. This difference will be asymptotic to the second exponential if $k/n > \mathcal{S}_1(p)$, and to the solution that corresponds to rays from the origin if $k/n < \mathcal{S}_1(p)$.

Consider first $p_* < p < 1$, where the secondary reflection occurs. While $A^n B^k$ satisfies the boundary condition along the n-axis, the second exponential does not. However, it can be compensated for by a third exponential of the form $A_*^n B_*^k$. This boundary layer construction leads to the term proportional to δ in (46). The secondarily reflected rays have

$$\dot{n} = \frac{1-p}{A_*} - \frac{A_*}{B} = -1 + \frac{p}{2} - \frac{1}{2p} + \left(\frac{1}{2} + \frac{1}{2p}\right)\sqrt{1+2p+5p^2}, \quad (66)$$

and $\dot{k} = A_*/B_* - (1+p)B_*$. We can easily show that $\dot{k} > 0$ for $p > p_*$ and that $\dot{n} > 0$ always. It follows that the secondary reflections fill only the sector $k/n < \mathcal{S}_2(p)$ and hence no further reflections are possible. This suggests also that the compensation method cannot be carried out further. Indeed, even if we ignore completely the ray geometry, we can try to correct for the third exponential $A_*^n B_*^k$ by a fourth, of the form $\tilde{A}^n B_*^k$, near the k-axis. But then we would find

that

$$\tilde{A} = \frac{1-p}{2(1+p)}\left[1+3p+\sqrt{1+2p+5p^2}\right] \qquad (67)$$

and so $\tilde{A} > A$. Hence, the fourth exponential cannot serve as a boundary layer correction to the third.

Finally we discuss rays from the origin. Since by (53) these have Φ_n and Φ_k constant along a ray, we set $\Phi_n = \log(a)$ and $\Phi_k = \log(b)$. In view of the PDE (50) we have

$$3 = \frac{a}{b} + (1-p)\frac{1}{a} + (1+p)b. \qquad (68)$$

Integrating (52) then leads to $n = t[(1-p)/a - a/b]$ and $k = t[a/b - (1+p)b]$ so that a particular ray has the slope

$$\frac{k}{n} = \frac{a/b-(1+p)b}{(1-p)/a - a/b}. \qquad (69)$$

We can view (68) and (69) as two equations for the two unknowns a and b, which are both functions of $k/n \equiv R$. Then (54) integrates to $\Phi = n\log(a) + k\log(b)$ and hence $\mathrm{e}^{\Phi} = a^n b^k = [a(k/n)]^n[b(k/n)]^k$. We can eliminate b to obtain the cubic equation (47) for a. This equation has three real branches, which we plot in Figure 5 for $p = 0.5$. We see that one branch starts at $a(0) > 1$, and the branch with the smallest value of $a(0)$ becomes negative as k/n increases past 1. Thus we choose the middle branch, which has $a'(R) > 0$ and corresponds to $k/n > 0$ in (69).

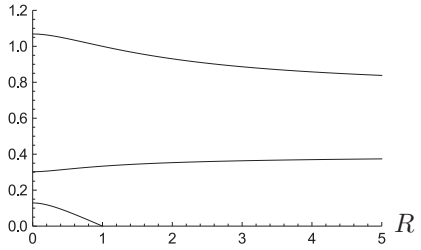

Fig. 5. The three branches of (47) for $R \in [0,5]$ and $p = 0.5$.

The rays from $(0,0)$ correspond to a non-product form solution in (49). For this solution Φ, we can rewrite, after some calculation, the transport equation (51) as $\dot{L}/L = -1/(2t)$, which gives the derivative of L along a ray. Hence we can write the general solution of L as $L = f(R)/\sqrt{n}$. It does not seem possible to determine the function $f(R)$ by ray-type analysis alone. Its determination would require a careful analysis of the "corner scale" $n, k = O(1)$, but this is equivalent to an exact solution to the full problem (obtained in [11]).

Rays from the origin thus lead to an asymptotic solution that is smaller than any of the three exponentials, but which fill the entire first quadrant for all values of p. This solution does not take into account the boundary conditions (2)-(5) along the axes. It is possible to construct boundary layer corrections to the ray solution, that will apply for $n \to \infty$, $k = O(1)$ and $k \to \infty$, $n = O(1)$. We omit that analysis, but comment that it would yield additional information about the function $f(R)$, namely that $f(R) \sim (\text{const.})R$ as $R \to 0$ and that $f(R) \sim (\text{const.}')R^{-3/2}$ as $R \to \infty$. The expansion that applies for $n \to \infty$ and $k = O(1)$ would have the form

$$n^{-3/2}(v_1 k + v_0)[a(0)]^n[b(0)]^k, \quad k \geq 1 \qquad (70)$$

with a suitable modification along $k = 0$. From (47) we also find that $a'(0) = 0$. For $k \to \infty$ and $n = O(1)$ the boundary layer correction to the ray expansion would take the form

$$k^{-3/2}(v_1' n + v_0')[b(\infty)]^k[a(\infty)]^n, \quad n \geq 1 \qquad (71)$$

and we have $b'(\infty) = 0$.

The asymptotic solution $n^{-1/2}f(R)[a(R)]^n[b(R)]^k$ will also develop problems near $R = k/n = \mathcal{S}_1(p)$ if $p < p_*$, and near $R = \mathcal{S}_2(p)$ if $p > p_*$, which corresponds to where an extra exponential begins to appear in the asymptotics. We omit the details of the analysis, but mention only that on the scale $k - n\mathcal{S}_1(p) = O(\sqrt{n})$ we can ultimately approximate the difference equation (1) by a parabolic PDE, from whose solution we can infer that $f(R)$ has a singularity of the form $f(R) \sim v_*[R - \mathcal{S}_1(p)]^{-1}$ as $R \to \mathcal{S}_1(p)$. We also note that $a(\mathcal{S}_1(p)) = A_*$ and $b(\mathcal{S}_1(p)) = B$, so that the rays from the origin and the exponential solution $A_*^n B^k$ agree along the critical line $R = \mathcal{S}_1(p)$, at least in their exponential orders of magnitude.

REFERENCES

[1] Adan, I.J.B.F. (1994). *A Compensation Approach for Queueing Problems*, CWI Tract 104, Mathematical Centre, Amsterdam.

[2] Adiz, A., D. Starobinski, P. Thiran (2009). Elucidating the instability of random wireless mesh networks. Submitted.

[3] De Bruijn, N.G. (1981). *Asymptotic Methods in Analysis*, Dover Publications, New York.

[4] Cohen, J.W. (1988). Boundary value problems in queueing theory. *Queueing Systems* **3**: 97-128.

[5] Cohen, J.W., O.J. Boxma (1983). *Boundary Value Problems in Queueing System Analysis*. North-Holland, Amsterdam.

[6] Fayolle, G., R. Iasnogorodski, V. Malyshev (1999). *Random Walks in the Quarter Plane*, Springer-Verlag, New York.

[7] Flajolet, P., R. Sedgewick (2009). *Analytic Combinatorics*, Cambridge University Press, Cambridge.

[8] Guillemin, F., D. Pinchon (2004). Analysis of generalized processor-sharing systems with two classes of customers and exponential services. *Journal of Applied Probability* **41**: 832-858.

[9] Guillemin, F., J.S.H. van Leeuwaarden (2009). Rare event asymptotics for a random walk in the quarter plane. Submitted for publication.

[10] Guillemin, F., C. Knessl, J.S.H. van Leeuwaarden (2009). Wireless multi-hop networks with stealing: large buffer asympotics. Longer report version. Downloadable from http://www.win.tue.nl/∼jleeuwaa/

[11] Guillemin, F., C. Knessl, J.S.H. van Leeuwaarden (2009). Wireless 3-hop mesh networks with stealing II: exact solutions through boundary value problems. Working paper.

[12] Gurewitz, O., V. Mancuso, J. Shi, E.W. Knightly (2009). Measurement and modeling of the origins of starvation of congestion-controlled flows in wireless mesh networks. *IEEE/ACM Transactions on Networking* **7**: 1832-1845.

[13] Kleinrock, L., F. Tobagi (1975). Packet switching in radio channels: part I - carrier sense multiple-access modes and their throughput-delay characteristics. *IEEE Transactions on Communications* **12**: 1400-1416.

[14] van Leeuwaarden, J.S.H., J.A.C. Resing (2005). A tandem queue with coupled processors: computational issues. *Queueing Systems* **51**: 29-52.

[15] Neuts, M.F. (1981). *Matrix-Geometric Solutions in Stochastic Models, An Algorithmic Approach*, The Johns Hopkins Press, Baltimore.

[16] Pemantle, R., M.C. Wilson (2008). Twenty combinatorial examples of asymptotics derived from multivariate generating functions. *SIAM Review* **50**: 199-272.